

# Synthesis of Well-Defined Poly(methyl methacrylate) Nanoparticles by Reverse Atom Transfer Radical Polymerization in a Microemulsion

Pan Kai, Dan Yi

State Key Laboratory of Polymer Materials Engineering, Polymer Research Institute, Sichuan University, Chengdu 610065, China

Received 9 February 2005; accepted 29 April 2005

DOI 10.1002/app.22792

Published online in Wiley InterScience (www.interscience.wiley.com).

**ABSTRACT:** Well-defined poly(methyl methacrylate) (PMMA) with an  $\alpha$ -isobutyronitrile group and an  $\omega$ -bromine atom as the end groups was synthesized by the microemulsion polymerization of methyl methacrylate (MMA) at 70°C with a 2,2'-azobisisobutyronitrile/CuBr<sub>2</sub>/2,2'-bipyridine system. The conversion of the polymerization reached 81.9%. The viscosity-average molecular weight of PMMA was high (380,000), and the polydispersity index was 1.58. The polymerization of MMA exhibited some controlled radical polymerization characteristics. The mechanism of con-

trolled polymerization was studied. The presence of hydrogen and bromine atoms as end groups of the obtained PMMA was determined by <sup>1</sup>H-NMR spectroscopy. The shape and size of the final polymer particles were analyzed by scanning probe microscopy, and the diameters of the obtained particles were usually in the range of 60–100 nm. © 2006 Wiley Periodicals, Inc. *J Appl Polym Sci* 101: 3670–3676, 2006

**Key words:** atom transfer radical polymerization (ATRP); atomic force microscopy (AFM); kinetics (polym.)

## INTRODUCTION

Since Szwarc<sup>1</sup> first reported anionic living polymerization, which realized truly living polymerization (without chain transfer and chain termination), much effort has been expended to find a living radical polymerization system<sup>2,3</sup> because radical polymerization plays a significant role in industrial processes. In recent years, several methods, such as nitroxide-mediated stable free-radical polymerization,<sup>2,4</sup> atom transfer radical polymerization (ATRP),<sup>3,5–8,10,11–15</sup> and reversible addition–fragmentation chain transfer,<sup>9</sup> have been developed for the living radical polymerization process.

ATRP is a versatile technique for the synthesis of well-defined polymers with various architectures (e.g., block, graft, and star polymers)<sup>5,16,17</sup> and narrow molecular weight distributions. However, ATRP has two major problems in the initiation system: the halide species RX is usually toxic, and the catalyst is easily oxidized by the oxygen in air. To overcome these

drawbacks, so-called reverse ATRP has been explored. In this process, a conventional radical initiator and a higher oxidation state transition-metal catalyst complex are used instead of the organic halide initiator RX and the lower oxidation state catalyst complex.

Although many studies have been reported about reverse ATRP,<sup>15,18</sup> most of the polymerizations have been confined to bulk or solution polymerization. Few well-defined polymers have been synthesized with emulsions or microemulsions. In this article, we report the synthesis of well-defined poly(methyl methacrylate) (PMMA) in a microemulsion, with  $\omega$ -bromine atom end groups and a high molecular weight, with the initiation system 2,2'-azobisisobutyronitrile (AIBN)/CuBr<sub>2</sub>/2,2'-bipyridine (bpy). The particles of the resultant PMMA were global, and the diameters of the particles were usually in the range of 60–100 nm.

## EXPERIMENTAL

### Materials

Methyl methacrylate (MMA) was purchased from Chengdu Kelong Chemical Reagent Factory (Chengdu, China) and was distilled under reduced pressure before use. CuBr<sub>2</sub>, chloroform, and *n*-hexanol all came from Chengdu Kelong Chemical Reagent Factory and were used directly. AIBN (analytical reagent) was obtained from Beijing Chemical Reagent Factory (Beijing, China) and was recrystallized from methanol before use. Hydroquinone (analytical re-

Correspondence to: D. Yi.

Contract grant sponsor: National Natural Science Foundation of China; contract grant number: 20374036.

Contract grant sponsor: Research Foundation of Sichuan Province; contract grant number: 03JY029-054-1.

Contract grant sponsor: Talent Training Foundation of Sichuan Province.

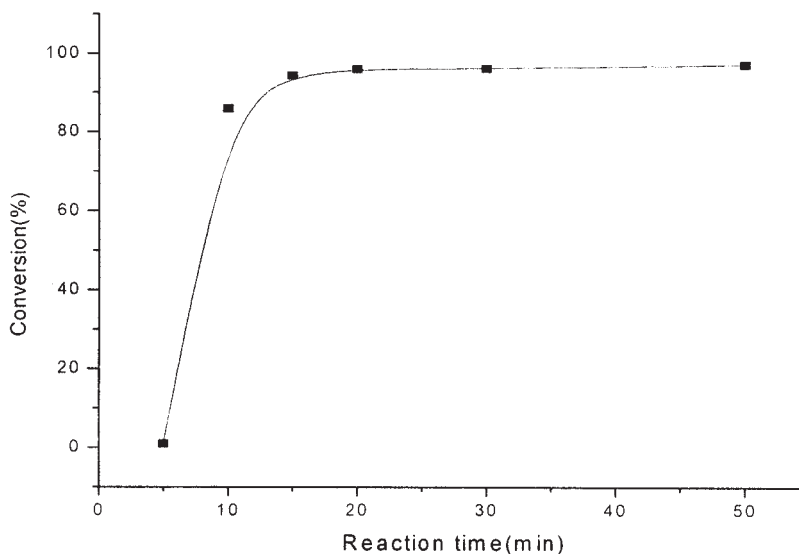


**Figure 1** Dependence of the conversion of MMA on the reaction time at 70°C without a catalyst [CuBr<sub>2</sub>/bpy; MMA/AIBN = 387/1 (molar ratio)].

agent) was purchased from Chengdu Reagent Factory (Chengdu, China). Sodium lauryl sulfate (SLS) was purchased from Chengdu Kelong Chemical Reagent Factory and was used directly. bpy (analytical reagent) came from Beijing Shiyong Chemical Reagent Factory (Beijing, China) and was used directly. Deionized water was used for all experiments.

#### Normal polymerization of MMA in a microemulsion

A 500-mL flask equipped with a magnetic stirrer was charged with deionized water, MMA, SLS, AIBN, and *n*-hexanol [MMA/SLS/AIBN/*n*-hexanol = 387/54/1/28 (molar ratio)] and stirred for 1 h at room temperature; then, the flask was immersed in a water bath

at 70°C. The reaction was carried out with stirring for 50 min. Samples were taken periodically via a syringe to monitor the conversion and molecular weight.

#### Reverse ATRP of MMA in a microemulsion

Reverse ATRP research can be found in articles, but many reverse ATRPs are carried out in bulk or solution systems. For example, Liu and Hu<sup>12</sup> used AIBN as an initiator and 1,10-phenanthroline as a ligand ([AIBN] = 0.047M, [CuCl<sub>2</sub>] = 0.094M, [phen] = 0.188M, [MMA] = 9.04M, acetonitrile = solvent, temperature = 70°C) and realized the reverse ATRP of MMA. The molecular weight of MMA increased linearly with an increase in the conversion; the final conversion was close to 100%, and the molecular weight was close to 10,000.

A 500-mL flask equipped with a magnetic stirrer was charged with MMA, CuBr<sub>2</sub>, bpy, and *n*-hexanol [MMA/CuBr<sub>2</sub>/bpy/*n*-hexanol = 387/1/2/28 (molar ratio)] and deoxygenated by vacuum/nitrogen cycles before the reaction, and the monomer solution was stirred at 60°C for 1 h. A 250-mL flask was charged with 200 mL of deionized water, SLS, and AIBN (SLS/AIBN = 54/1) and deoxygenated three times. At room temperature and under a nitrogen atmosphere, the surfactant solution was stirred for 0.5 h and added to the monomer solution under nitrogen, and then the flask was immersed in a water bath at 70°C. The reaction was carried out with stirring and under nitrogen for 3 h. Samples were taken periodically via a syringe to monitor the conversion and molecular weight.

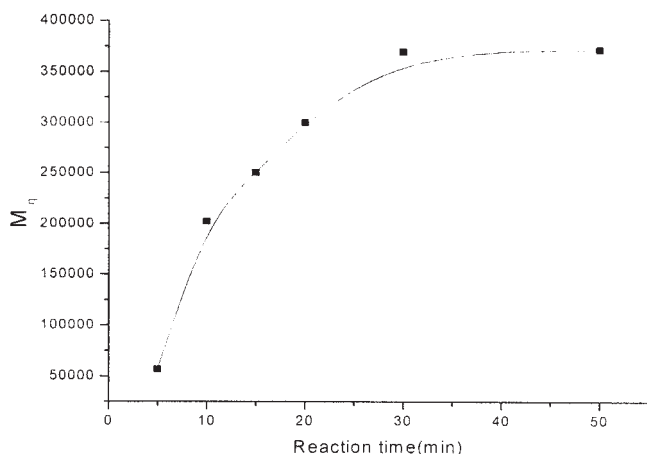


**Figure 2** Dependence of  $M_n$  of PMMA on the reaction time without a catalyst [CuBr<sub>2</sub>/bpy; MMA/AIBN = 387/1 (molar ratio)].

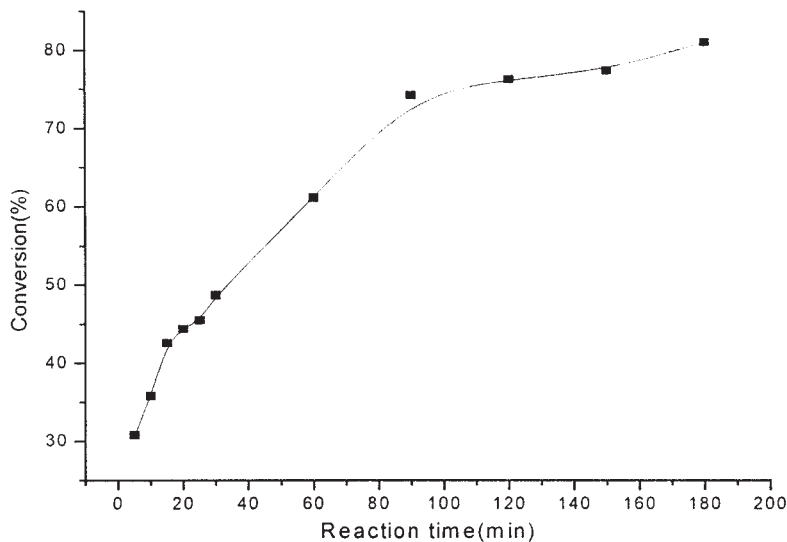


**Figure 3** Dependence of the conversion of MMA on the time at 70°C with a catalyst [CuBr<sub>2</sub>/bpy; MMA/AIBN/CuBr<sub>2</sub>/bpy = 387/1/1/2 (molar ratio)].

### Measurements

The conversion of the polymers was measured by a weighting method. The viscosity-average molecular weight ( $M_\eta$ ) of the polymers was determined at 30°C with an Ubbelohde viscometer with CHCl<sub>3</sub> as a solvent and was calculated with the equation<sup>19</sup>  $[\eta] = KM_\eta^\alpha$ , where  $[\eta]$  is the intrinsic viscosity,  $K$  is 0.0043 mL/g, and  $\alpha$  is 0.80. The molecular weight distributions of the polymer samples were measured at 35°C by gel permeation chromatography (GPC) on a Waters 2410 instrument with tetrahydrofuran as the solvent (1.0 mL/min), with calibration with polystyrene standards, and with Waters Millennium 32 as the data-processing software. An ultraviolet-visible (UV-vis)

light photometer was used to measure the absorbance of the CuBr<sub>2</sub>/bpy complex. <sup>1</sup>H-NMR spectra were taken at 25°C on a Bruker ARX400 (400 MHz) spectrometer in CDCl<sub>3</sub> with tetramethylsilane as an internal reference. The shape and size of the final polymer particles were analyzed with an SPA 400 scanning probe microscope from Seiko Instruments, Inc.

## RESULTS AND DISCUSSION

### Polymerization of MMA in a microemulsion

First, the normal microemulsion polymerization of MMA initiated with AIBN was carried out at 70°C [MMA/SLS/AIBN/*n*-hexanol = 387/54/1/28 (molar ratio)]. The results are shown in Figures 1 and 2. Figure 1 shows that the conversion of MMA quickly reached 85.9% within 10 min once the polymerization began. Then, the conversion increased slowly from 85.9 to 96.9% within 50 min. Figure 2 shows the relation between  $M_\eta$  and the reaction time; with an increase in the reaction time,  $M_\eta$  of PMMA increased quickly within 30 min, reaching 369,490, and then  $M_\eta$  increased less in the rest of the time. The results agreed well with the kinetic of radical polymerization. On the basis of the kinetics of radical polymerization, we know that the chain propagating activation energy was low, so the rate of chain growth was fast, and the molecular weight quickly propagated in a few minutes. With the propagation of the radical chain, the particle size increased, and the propagating center was wrapped further; the new radical entering the micelle could not react with it, and then the new radical became a new propagating center and propagated continually. Therefore, the average molecular

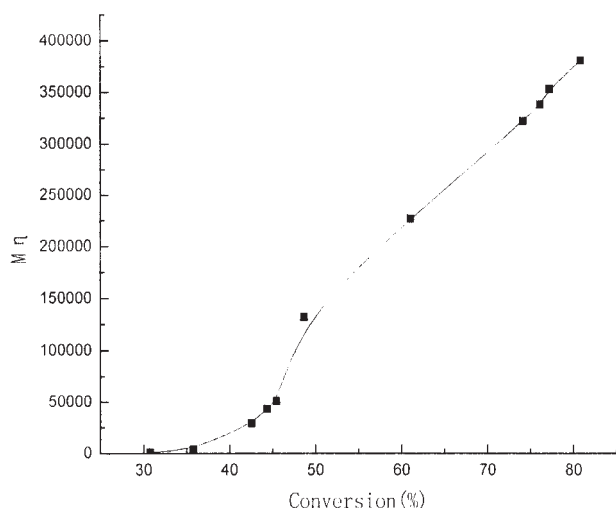


**Figure 4** Dependence of  $M_\eta$  of PMMA on the conversion with a catalyst [CuBr<sub>2</sub>/bpy; MMA/AIBN/CuBr<sub>2</sub>/bpy = 387/1/1/2 (molar ratio)].

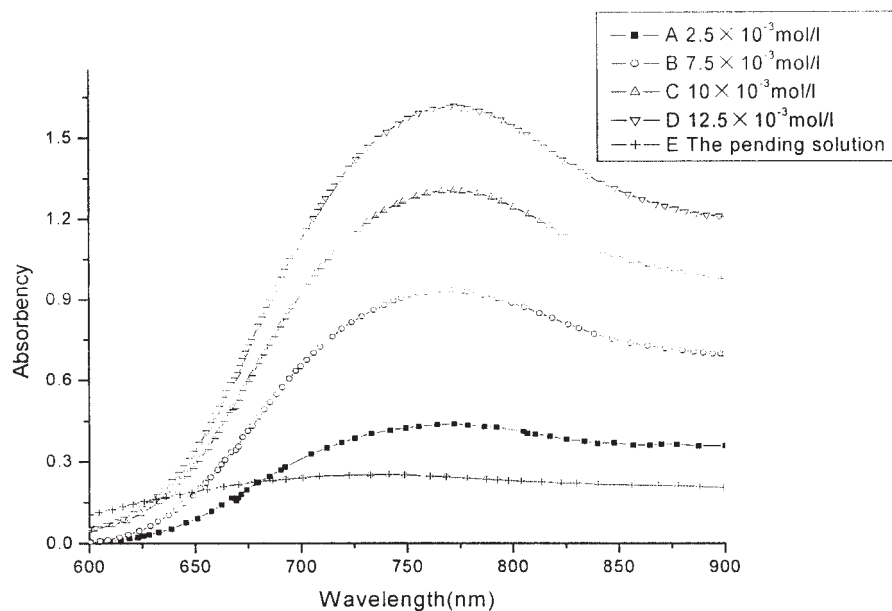


**Figure 5** Absorbance of  $\text{CuBr}_2/\text{bpy}$  complex solutions. Lines A–D are the absorbance of  $\text{CuBr}_2/\text{bpy}$  complex solutions of known concentrations; line E is the absorbance of the pending solution in a water phase.

weight increased slowly in the rest of the time of polymerization.

The whole process was obviously uncontrolled. The molecular weight distribution of the resultant polymer was measured by GPC, and the polydispersity index was 1.90.

The reverse ATRP of MMA in a microemulsion with the AIBN/ $\text{CuBr}_2/\text{bpy}$  system (MMA/AIBN/ $\text{CuBr}_2/\text{bpy} = 387/1/1/2$ ) was carried out at  $70^\circ\text{C}$ , and the results are shown in Figures 3 and 4. Figure 3 shows that the conversion of MMA increased slowly with increasing time, in comparison with Figure 1. Figure 3 also shows that the conversion reached only 35.8% within 10 min and 61.1% within 60 min. After 180 min

of polymerization, the conversion reached 80.9%. The reason is that the concentration of the growing species was controlled (to form a dormant species with the  $\text{CuBr}_2/\text{bpy}$  complex), and the rate of polymerization slowed down in comparison with Figure 1. Figure 4 shows the relationship between  $M_n$  and the conversion for the reverse ATRP of MMA when the AIBN/ $\text{CuBr}_2/\text{bpy}$  molar ratio was 1 : 1 : 2. Figure 4 shows that  $M_n$  increased uncontrollably with an increase in the conversion before 133,392, and then  $M_n$  increased linearly (from 133,392 to 381,850) with an increase in the conversion; this is quite different from the situation in Figure 2. The reason might be that the microemulsion system was multiphase in comparison with

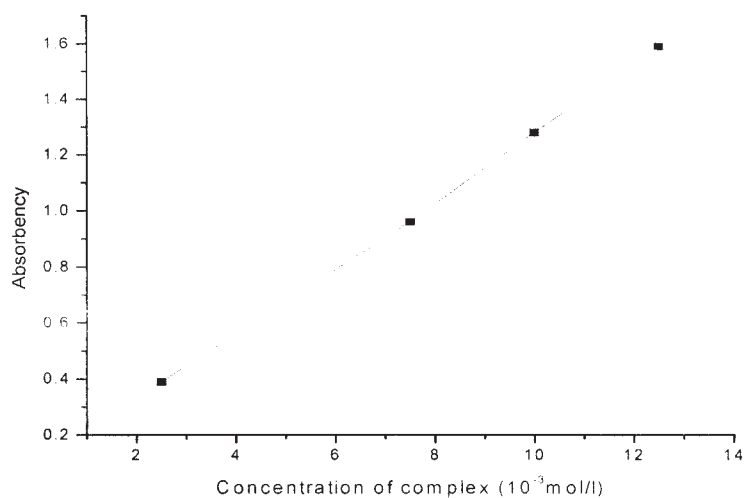


**Figure 6** Dependence of the absorbance on the concentration of the  $\text{CuBr}_2/\text{bpy}$  complex solution.

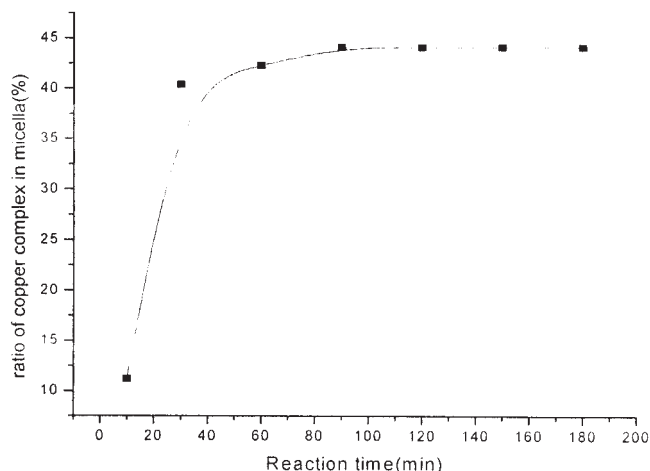


**Figure 7** Dependence of the ratio of the complex in the oil phase on the time.

the bulk system. When the reaction began, time was needed for the  $\text{CuBr}_2/\text{bpy}$  complex to react with a radical to form a dormant species. During this process, the polymerization was uncontrolled. When atom transfer equilibrium was established in the polymerization process, the concentration of the propagating radical was kept at a constant level, so the process was a controlled polymerization. In our designed experiment (see the next section), the ATRP process in a microemulsion could be clearly observed. The molecular weight distribution of the resultant PMMA was also measured by GPC. The polydispersity index was 1.58.

### Controlled polymerization mechanism

As we know, in ATRP, there are two reversible dynamic equilibria: the complex equilibrium of  $\text{CuBr}_2/\text{bpy}$  and the active/reactive equilibrium of the radical. The controlled polymerization mechanism of ATRP in a microemulsion is more complicated than that in bulk because the microemulsion system is multiphase in comparison with the bulk system.  $\text{CuBr}_2$  is easily dissolved in a water phase, and  $\text{bpy}$  is easily dissolved in an oil phase. Only  $\text{CuBr}_2$  complexes with  $\text{bpy}$ , and then the  $\text{CuBr}_2/\text{bpy}$  complex reacts with the radical, so the concentration of the radical can be controlled. The radical polymerization is controlled by the control of the concentration of the radical. We do not clearly know whether  $\text{bpy}$  moves from the oil phase to the water phase and then complexes with  $\text{CuBr}_2$  or  $\text{CuBr}_2$  moves from the water phase to the oil phase and then complexes with  $\text{bpy}$ , but we can measure the ratio of the complex in the oil phase with our designed experiment. Because only the complexes enter the oil phase, they can react with the radical and reach the active/reactive equilibrium to control the concentration of the radical. Therefore, the ratio of the complex presents the efficiency of the catalyst ( $\text{CuBr}_2/\text{bpy}$ ).

Figure 5 shows the absorbance of  $\text{CuBr}_2/\text{bpy}$  complex solutions measured with a UV-vis light photometer. The real line is the absorbance of a  $\text{CuBr}_2/\text{bpy}$  complex solution of a known concentration, and the broken line is the absorbance of the pending solution in a water phase, which was charged with water,

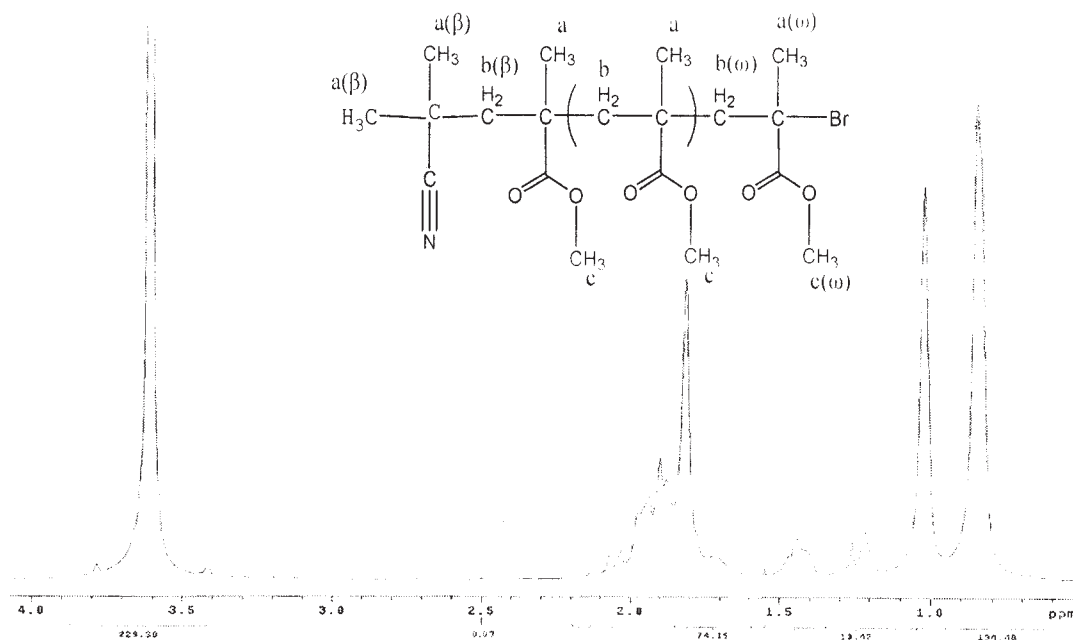


**Figure 8**  $^1\text{H}$ -NMR spectrum ( $\text{CDCl}_3$ , 400 MHz) of PMMA (weight-average molecular weight/number-average molecular weight = 1.58) synthesized with the  $\text{AIBN}/\text{CuBr}_2/\text{bpy}$  system in a microemulsion.

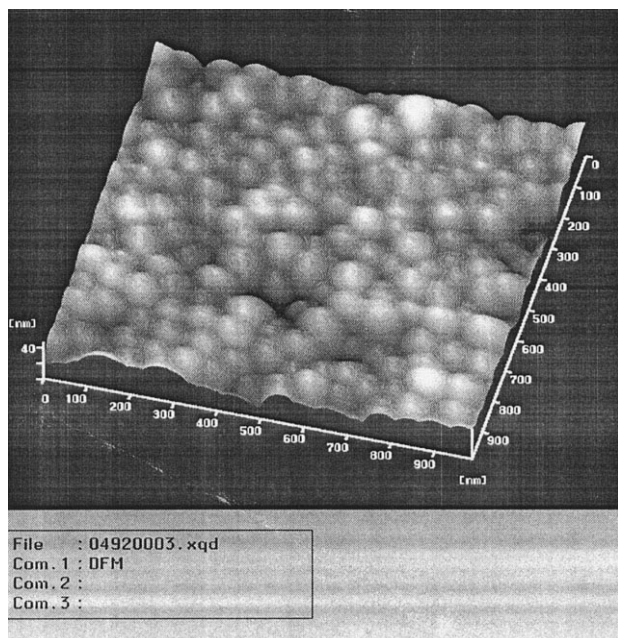


**Figure 9** Scanning probe microscopy image of the final polymer particles ( $M_n = 380,000$ , weight-average molecular weight/number-average molecular weight = 1.58).

MMA,  $\text{CuBr}_2$ , bpy, SLS, and *n*-hexanol and stirred for a definite time at  $70^\circ\text{C}$  in a water bath. Figure 6 shows the linear correlation of the absorbance with the concentration of a  $\text{CuBr}_2/\text{bpy}$  complex solution. From Figures 5 and 6, we can obtain the ratio of the  $\text{CuBr}_2/\text{bpy}$  complex between the water phase and oil phase. Figure 7 shows the changing correlation of the ratio of the complex in the oil phase with the time. The ratio of the complex in the oil phase reached only 11.2% after 10 min of reaction, and the ratio reached 44.1% after 90 min of reaction; then, the ratio remained stable with increasing time. However, the ratio was still low; improving it requires research.

### End-group analysis

An end-group analysis of the resultant PMMA was carried out with  $^1\text{H-NMR}$  spectroscopy. Figure 8 shows a representative  $^1\text{H-NMR}$  spectrum of well-defined PMMA. The spectrum is the same as that reported by Chen and Qiu.<sup>20</sup> The signals at 0.84–1.21, 1.81–1.90, and 3.60 ppm were assigned to the protons of the methyl groups (peak a) of  $-\text{C}(\text{CH}_3)(\text{COOCH}_3)$ , methylene groups (peak b) of  $-\text{CH}_2-$ , and methoxy groups (peak c) of  $-\text{C}(\text{CH}_3)(\text{COOCH}_3)$ , respectively. These results suggested that the chains of PMMA had only methyl groups and methylene groups. The signal at 1.44 ppm [peak a( $\beta$ )] was for the methyl groups, and the signal at 1.54 ppm [peak b( $\beta$ )] was for the

methylene protons. This indicated that one end group of the PMMA chain was an  $\alpha$ -isobutyronitrile group [ $-\text{C}(\text{CN})(\text{CH}_3)_2$ ]. In particular, the signal at 3.79 ppm [peak c( $\omega$ )] was for the protons of the methoxy group, that at 2.50 ppm [peak b( $\omega$ )] was for the methylene protons, and that at 2.07 ppm [peak a( $\omega$ )] exhibited the characteristic chemical shifts of the terminal MMA unit capped with an  $\omega$ -end bromine. Thus, an  $\omega$ -end bromine atom end group was just another end group.

### Scanning probe microscopy analysis of resultant PMMA particles

Scanning probe microscopy analysis tends to observe the shape and measure the size of final polymer particles. Figure 9 presents a three-dimensional image of the final polymer particles. It shows that plenty of PMMA latex particles were packed together, but the shapes of the particles were well kept. Figure 9 also shows that the diameters of the particles had a narrow distribution.

Therefore, the polymers produced with the initiation system were well defined, having not only a high molecular weight but also precise end groups, that is,  $\alpha$ -isobutyronitrile groups and  $\omega$ -bromine atoms. The shapes of the final polymer particles were global, and the diameters of the particles were 60–100 nm.

## CONCLUSIONS

A reverse ATRP was performed with the AIBN/ $\text{CuBr}_2/\text{bpy}$  system for the controlled radical polymerization of MMA in a microemulsion at  $70^\circ\text{C}$ . A well-defined PMMA with a high molecular weight (up to 380,000) was obtained with this system. The controlled mechanism was studied. The  $^1\text{H-NMR}$  spectra revealed the presence of an  $\omega$ -end bromine atom end group from the catalyst. The final polymer could be used as a macroinitiator to initiate chain-extension polymerization via the conventional ATRP process. A scanning probe microscopy image showed that the shapes of the final polymer particles were global and that the diameters of the particles were 60–100 nm.

### References

1. Szwarc, M. *Nature* 1956, 178, 1168.
2. Georges, M. K.; Veregin, R. P. N.; Kazmaier, P. M.; Hamer, G. K. *Macromolecules* 1993, 26, 2987.
3. Kato, M.; Kamigaito, M.; Sawamoto, M.; Higashimura, T. *Macromolecules* 1995, 28, 1721.
4. Odell, P. G.; Veregin, R. P. N.; Michalak, L. M.; Brousmiche, D.; Georges, M. K. *Macromolecules* 1995, 28, 8453.
5. Wang, J. S.; Matyjaszewski, K. *Macromolecules* 1995, 28, 7901.
6. Percec, V.; Barboiu, B. *Macromolecules* 1995, 28, 7970.
7. Qiu, J.; Gaynor, S. G.; Matyjaszewski, K. *Macromolecules* 1999, 32, 2872.

8. Wan, X.; Ying, S. *J Appl Polym Sci* 2000, 75, 802.
9. Chiefari, J.; Chong, Y. K.; Ercole, F.; Krstina, J.; Jeffery, J.; Le, T. P. T.; Mayadunne, R. T. A.; Meijs, G. G.; Moad, C. L.; Moad, G.; Rizzardo, E.; Thang, S. H. *Macromolecules* 1998, 31, 5559.
10. Matyjaszewski, K.; Wei, M. L.; Xia, J. H.; McDermott, N. E. *Macromolecules* 1997, 30, 8161.
11. Jousset, S.; Qiu, J.; Matyjaszewski, K. *Macromolecules* 2001, 34, 6641.
12. Liu, B.; Hu, C. P. *Eur Polym J* 2001, 37, 2025.
13. Paik, H. J.; Matyjaszewski, K. *Polym Prepr* 1996, 37, 274.
14. Matyjaszewski, K.; Jo, S. M.; Paik, H. J.; Shipp, D. A. *Macromolecules* 1999, 32, 6531.
15. Matyjaszewski, K.; Nakagawa, Y.; Jasieczek, C. B. *Macromolecules* 1998, 31, 1535.
16. Zhang, Z. B.; Ying, S. K.; Shi, Z. Q. *Polymer* 1999, 40, 1341.
17. Wang, X. S.; Luo, N.; Ying, S. K. *Polymer* 1999, 40, 4515.
18. Qin, D. Q.; Qin, S. H.; Qiu, K. Y. *J Appl Polym Sci* 2001, 81, 2237.
19. Yu, Z. G. *Measurement of Polymer Molecules*; Shanghai Science and Technology: Shanghai, 1984.
20. Chen, X. P.; Qiu, K. Y. *Macromolecules* 1999, 32, 8711.